The 8th European Congress on Computational Methods in Applied Sciences and Engineering
ECCOMAS Congress 2022
5-–9 June 2022, Oslo, Norway

HIGH FIDELITY FLUID-STRUCTURE INTERACTION SIMULATION OF A MULTI-MEGAWATT AIRBORNE WIND ENERGY REFERENCE SYSTEM IN CROSSWIND FLIGHT

Niels Pynaert[1,2], Jolan Wauters[1,2], Guillaume Crevecoeur[1,2] and Joris Degroote[1,2]

[1] Department of Electromechanical, Systems and Metal Engineering
Faculty of Engineering and Architecture
Ghent University
Sint-Pietersnieuwstraat 41, 9000 Gent, Belgium
e-mail: {Niels.Pynaert, Jolan.Wauters, Guillaume.Crevecoeur, Joris.Degroote}@UGent.be

[2] Core lab EEDT, Flanders Make, Belgium

Key words: Airborne wind energy, Fluid-structure interaction, Chimera

Abstract. Airborne wind energy (AWE) is an emerging technology for the conversion of wind energy into electricity by flying crosswind patterns with a tethered aircraft connected to a generator either on board or on the ground. Having a proper understanding of the unsteady interaction of the air with the flexible and dynamic system during operation is key to developing viable AWE systems. The research goal is to simulate the time-varying fluid-structure interaction (FSI) of an AWE system in a crosswind flight maneuver using high fidelity simulation tools. In this work a framework is presented that serves as a proof of concept to perform high fidelity simulations of airborne wind energy systems. This is done using a partitioned and explicit approach in the open-source coupling tool CoCoNuT. An existing finite element method (FEM) model of the wing structure is coupled with a newly developed computational fluid dynamics (CFD) model of the wing aerodynamics including rigid body motion. It has been found that the mesh deformation is quite sensitive to dynamic mesh parameters. On the other hand, the overset/Chimera technique has been proven to be a robust approach to simulate the motion of an AWE system in CFD simulations.

1 INTRODUCTION

Airborne wind energy (AWE) is an emerging technology for the conversion of wind energy into electricity by flying crosswind patterns with a tethered aircraft. Currently, different types of AWE systems exist. A distinction can be made between soft kites or fixed wings and whether energy conversion takes place on board or on the ground [1]. The focus of the presented research is on fixed-wing aircraft systems with on-ground conversion. As indicated in [2], tests have shown that a proper understanding of the unsteady interaction of the air with the dynamic system during operation is key to developing viable AWE systems. Examples of unsteady aerodynamic phenomena that can arise during the operation of an AWE system are flutter or other unsteady fluid-structure interactions (FSI), the unsteady motion (e.g. varying velocity) of the aircraft, wake interactions, turbulence and gusts. High-fidelity simulation tools based on computational fluid dynamics (CFD) are needed to predict these phenomena and will provide insight into the design and operation of advanced and efficient AWE systems. In this work, a framework is presented that allows simulating these unsteady phenomena using high fidelity tools. The focus of this paper is on fluid-structure interaction.

Aeroelastic optimization of morphing AWE wings has been performed in [3]. This work is currently the only fixed-wing AWE model which combines FSI simulations with control and flight dynamics. The analysis method considers a two-way weakly coupled 3D static aeroelastic analysis model using a low-fidelity method and a 3D finite element model. A validated aeroelastic model of a large airborne wind turbine is developed in [4] and the aeroelastic effect of two bridle lines is analyzed in detail. The developed model is an extension of ASWING (aerodynamic, structural and flight dynamic model for flexible aircraft). ASWING allows a lifting-line 3D representation with an unsteady flow model. In that analysis, however, only a horizontal steady flight is considered without relevant flight dynamics. An aero-structural model for a composite swept wing (semi-rigid) is developed in [5], with the goal of design space exploration. A structural model using Timoshenko beam theory is coupled with a non-linear vortex lattice method (VLM). Current research in fluid-structure interaction for AWE is rather limited and a steady wind profile is assumed in the state-of-the-art techniques. Except for reference [3], flight conditions for the FSI models are steady and horizontal. This is in contrast to the field of horizontal-axis wind turbines, where unsteady high fidelity FSI simulation techniques have been developed [6]. High fidelity aerodynamic models for AWE systems are developed in [7] and [8], but these consider steady aerodynamics, without taking into account the dynamic motion of AWE systems or other unsteady effects. In [9] the dynamic motion is considered, but the modeling of the aerodynamic forces of the aircraft is limited to an analytical formulation of the aerodynamic coefficients.

In this work, a framework is developed that couples the structural model presented in [10] with an own developed computational fluid dynamics (CFD) model of the reference model geometry [10]. This is done using CoCoNuT, an open-source coupling code for numerical tools, developed by the fluid mechanics team at Ghent University. Different coupling techniques are used in this work. For the steady FSI, a fictive time step is introduced and iterations are performed between the steady aerodynamic and structural model until convergence is reached. For the unsteady FSI, an explicit approach is taken, evaluating the unsteady aerodynamic and structural model once per time step. Within the CFD model, the Chimera/overset technique is used to couple the wing component mesh with the atmospheric boundary layer mesh. This technique allows taking into account large rigid body motion while maintaining a constant mesh quality. The Chimera/overset technique has been proven successful for horizontal axis wind turbines in [6], but requires new developments to be applicable for AWE as the motion is much more dynamic.

The outline of this paper is as follows. The methodology is explained in section 2. Results are explained in section 3. Finally, section 4 provides the conclusions and an outlook to future work.

2 METHODOLOGY

The outline of the methodology is as follows. The aircraft design used in this paper is described in section 2.1. The fluid-structure interaction model, which will couple the structural and aerodynamic model is described in section 2.2. The description of the flight path is discussed in section 2.3.

2.1 Reference model

In [10], a complete model of a multi-megawatt AWE system is described that is used for this work. The design of this reference system aircraft is visualized in Figure 1. An AWE system consists of different components being an aircraft, a ground station, and a tether to connect the aircraft with the ground station. With a wing area of 150 m^2, the AWE system is designed to reach a power output in the order of 5 MW.

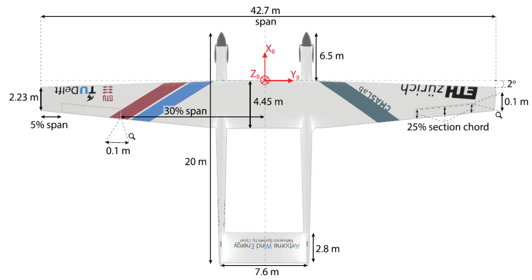

Figure 1: Multi-MW AWE reference system [10].

2.2 Fluid-structure interaction model

For the fluid-structure interaction model a partitioned approach is used, a schematic of this approach is given in Figure 2. In a fluid-structure interaction problem, the aerodynamic forces depend on the structural state. The structural state depends in turn on the aerodynamic loads being pressure and friction. In this work, frictional forces are neglected. The contribution of frictional forces to the deformation of the structure is assumed negligible. This partitioned FSI approach is provided by the open-source python code CoCoNuT, a coupling code for numerical tools [11]. The main ingredients of this approach are the aerodynamic and structural model, interpolation and coupling algorithm. For the aerodynamic model and structural model, computational fluid mechanics and structural mechanics are used. The rigid-body motion in the aerodynamic model is determined by a newly developed module in CoCoNuT and applies the motion to the wing component mesh. For now, the rigid-body motion is not included in the structural model but will be included in later work. Therefore, inertial and gravitational forces are neglected in the structural model. The effect of these forces on the structural deformation is assumed to be small, but this will be verified in later work. Solver wrappers have been developed in CoCoNuT, to enable communication with the CFD and CSM software. The loads resulting from the aerodynamic model and deformation from the structural model are evaluated at the FSI-interface, which is the wing surface. Interpolation is required at this surface to transfer this information from one mesh to the other. Finally, a coupling algorithm is required that determines the output obtained from one solver to determine the input for the other solver and to determine when the iterations between the two solvers can stop.

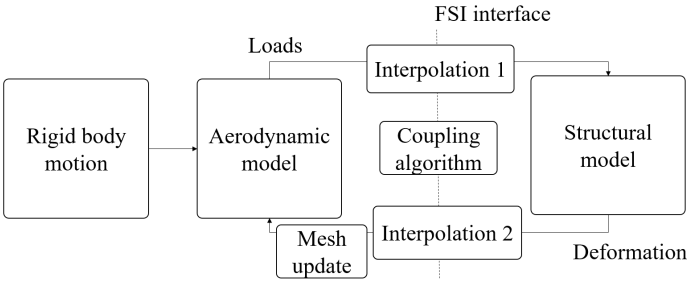

Figure 2: Partitioned FSI approach

2.2.1 Structural model

The Nastran structural model is obtained from the reference model [10] and converted to an Abaqus model. This is a FEM model of the composite wing consisting of skin, spars and ribs using shell elements. The stringers, fuselage and tail are modeled using beam elements (see Figure 3). Note that these structural elements are not included in the aerodynamic model. The aircraft is clamped in the middle at the spars (indicated in red) and is subjected to the aerodynamic loading (pressure) on the main wing. Both steady and unsteady models are used.

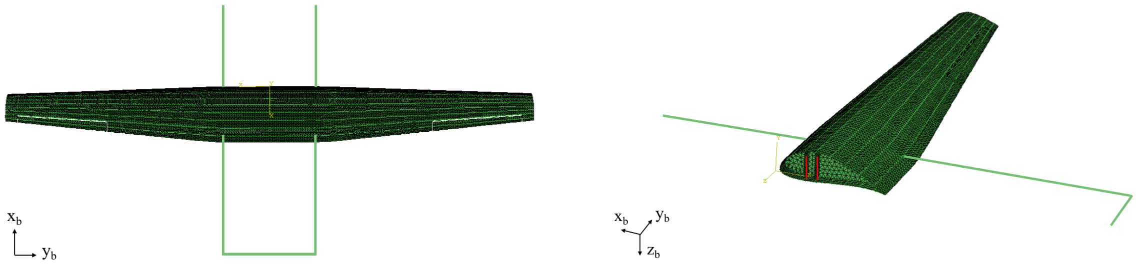

Figure 3: Structural model and cross-section

2.2.2 Aerodynamic model

An aerodynamic model of the wing of the reference aircraft is developed using computational fluid dynamics (CFD) to predict the aerodynamic loads on the wing. The model is built such that both flexible motion and rigid body motion of the wing can be taken into account. The tail and fuselage are not considered in the aerodynamic model, as the contribution of these elements to the aerodynamic loads is assumed small. A description of the domain, mesh and solver settings is given in this section.

Wing component mesh - A structured mesh with C-topology has been developed to capture the flow close to the aircraft wing (see Figure 4). This mesh consists of 6.4e6 cells and has an average y-plus value of 50 at the wing surface. This mesh serves as a proof of concept, a detailed grid sensitivity analysis will be done in future work.

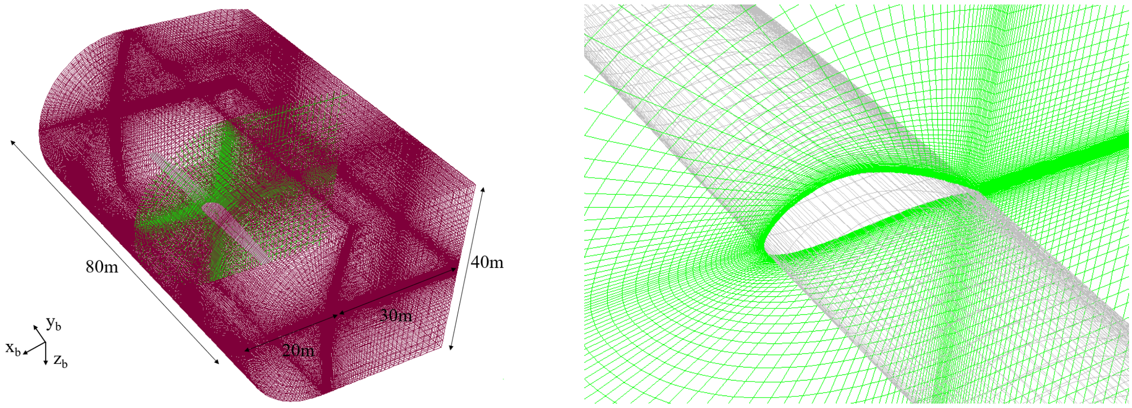

Figure 4: Wing component mesh. Purple: component mesh (overset) boundary, green: internal intersection, grey: wing surface [12].

Dynamic mesh - The wing component mesh should be able to deform according to structural deformations on the wing surface. To do this the arbitrary Lagrangian-Eulerian (ALE) formulation is used. This means that the mesh at the interface moves with the structure, while the internal mesh of the CFD model is moving arbitrarily, unrelated to structure or aerodynamics. A diffusion equation (eq. 1) is used to calculate the mesh deformation velocity $\vec{u}$. The diffusion is based on the normalized boundary distance (d) from the wing surface. It has been found that the quality of the deformed mesh is sensitive to dynamic mesh parameters.

$$\nabla \cdot (\frac{1}{d} \nabla \vec{u}) = 0 \tag{1}$$

Atmospheric boundary layer mesh - To simulate a crosswind flight maneuver, a Cartesian background is created to simulate atmospheric wind conditions. A large computational domain is required which encompasses the complete flight trajectory of the AWE system, including a margin to allow for the development of the wake and induced flow. The mesh that is developed to represent the atmospheric boundary layer (ABL) is visualized in Figure 5. The size of this domain is determined by providing 5 times the diameter of the aircraft's circular path in front and above this path and 10 times this diameter behind. This is based on rules of thumb for conventional wind turbine simulation [13]. Inside this large domain, mesh refinement is applied in a cuboid with dimensions 620x620x100m that is centered around the flight path. Within this cuboid, the mesh consists of cubical cells with an edge size of 4m, which is 10% of the wing span. The total number of cells in the ABL mesh amounts to 7.3e6. In this proof of concept, the atmospheric boundary layer is simplified by a uniform inlet speed. Nevertheless, this model allows for more complex ABL representations such as a logarithmic wind profile, turbulent wind and gusts in future work.

Chimera/overset technique - The wing component mesh moves through the stationary ABL mesh according to the prescribed flight path. The Chimera/overset technique enables the coupling between the ABL flow and the flow near the wing, by interpolating overlapping cells while solving the flow equations. For good connectivity, it is required to have similar cell sizes at the overset boundary [6]. The types of cells are visualized in Figure 6. Green cells are solved

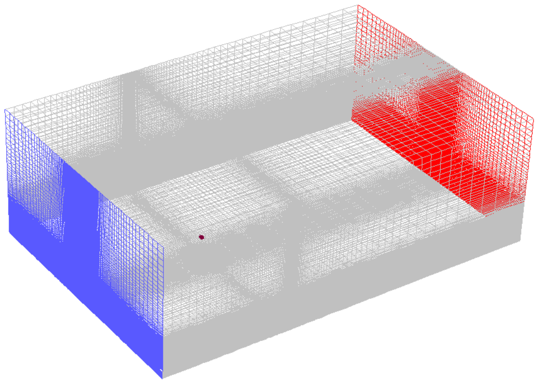

Figure 5: ABL mesh (2655m*5310m*7965m). Blue: velocity inlet, red: pressure outlet, grey: no slip wall, purple: overset boundary component mesh [12].

without interpolation. The large cells indicated in red are the donor cells of the background mesh. The solution of these cells is interpolated and passed to the outer blue receptor cells of the component mesh. The inner blue receptor cells of the background mesh get the interpolated solution from the donor cells of the component mesh. These are hidden below the blue receptor cells of the background mesh.

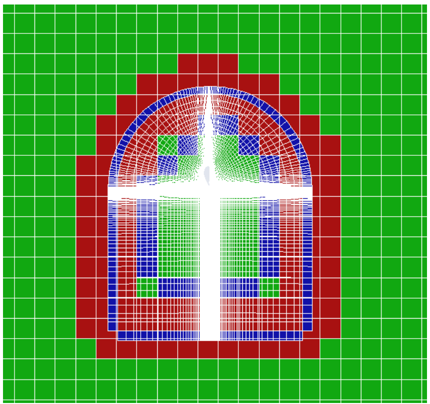

Figure 6: Chimera mesh connectivity. Green: solved cells, red: donor cells, blue: receptor cells [12].

Flow solver settings - The flow field is determined through incompressible unsteady Reynolds Averaged Navier-Stokes (URANS) simulations using the k-ω SST model and wall functions. Pressure-velocity coupling is realized using a coupled scheme. The convective terms in the momentum equations are discretized in space using a first-order upwind scheme and in time using a first-order implicit scheme. A time step of 0.005 seconds is chosen.

2.2.3 Interpolation

For the fluid and structural model different mesh topologies have been used which are most suitable for each independently. These meshes and nodes do not match and therefore interpolation at the interface is necessary. This is done using bilinear interpolation in barycentric coordinates using an existing algorithm in the CoCoNuT code.

2.2.4 Coupling algorithms

Different coupling algorithms are used in this work. A schematic of the algorithms is given in Figure 7, where **x** represents the output of the structural solver **S** (displacement at the interface), **y** the output of the fluid solver **F** (aerodynamic loads at the interface), k represents the iteration number, and n the time step.

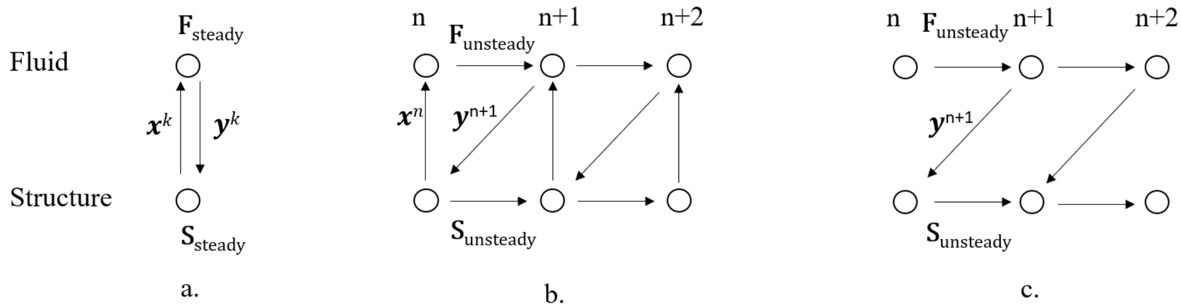

Figure 7: Schematic of coupling algorithms: a. Coupling of steady solvers, b. Explicit (two-way) coupling of unsteady solvers, c. One-way coupling of unsteady solver

For the steady FSI algorithm, the steady aerodynamic model and steady structural model are coupled by iterating the process of feeding the output of the structural solver to the fluid solver and vice versa until predefined convergence criteria are reached. An IQNI algorithm is used for the iteration process [14]. This algorithm is readily available in CoCoNuT.

For the unsteady FSI algorithms, an explicit approach is taken. This means that each solver is only evaluated once per time step (0.005 s). For comparison, a two-way and one-way approach are considered. In the two-way approach, the output of the structural model of the previous time step is used to evaluate the aerodynamic loads for the next time step. The output of the aerodynamic model of this time step is used to evaluate the structural displacement of the same time step. For the one-way coupling, the displacement is not fed back to the fluid solver.

2.3 Simulation of the in crosswind flight maneuver

The aircraft of an AWE system is subjected to very complex and dynamic movements. The flight path of the AWE system considered in this work is visualized in Figure 8. Two coordinate systems are defined in this figure: the global coordinate system, which is fixed to the ground, and the body-fixed coordinate system, which moves with the aircraft. The flight path is a vertical circle with a radius of 265.5 m and the center 403 m above the ground. The flight speed is a constant of 80 m/s. There is a uniform inlet velocity of 10 m/s imposed at the aerodynamic model to simulate incoming wind. The aircraft is pitched with an angle of -7.1°, to have an angle of attack of 0° with respect to the relative flow velocity. The implementation of the rigid body motion is explained in [12].

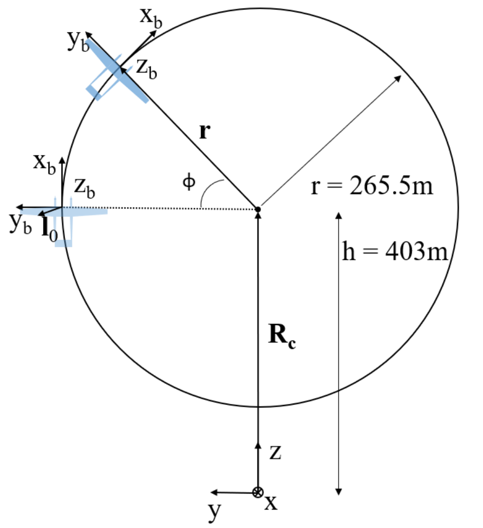

Figure 8: Flight path visualization [12].

3 RESULTS

The results for 2 flight conditions are presented in this section. In section 3.1, the results are presented for a steady horizontal flight condition. In section 3.2, the results are presented for a crosswind flight condition as defined in section 2.3.

3.1 Steady horizontal flight condition

For the horizontal flight condition a constant flight speed of 80 m/s and an angle of attack of 0° is simulated. The flight speed is imposed as an inlet-velocity boundary condition in the aerodynamic model of the wing component. The atmospheric model is not used for these results. The FSI simulations are initialized with a steady CFD simulation and an unloaded structure. the lift and drag coefficient versus time for the CFD only, steady FSI, and two-way and one-way FSI simulations are plotted in Figure 9. The coefficients predicted by the CFD only, steady FSI and unsteady FSI one-way simulations are invariant in time. This is trivial for the CFD only and steady FSI case, due to the steady nature. For the unsteady FSI 1-way approach, there is no feedback of structural deformation and there are currently no dynamic variations in inlet condition and flight velocity, so constant coefficients are expected. CFD only and unsteady FSI one-way predicts the same force coefficients as expected. The steady FSI simulation predicts a lift and drag coefficient, that is lower than predicted by the CFD model. For the lift coefficient there is a reduction of 1.4%. This is explained by the negative twist deformation of the wing (see Figure 11), which amounts -0.45°. For the two-way unsteady FSI simulation, the force coefficients are variant in time. Due to the oscillation of the wing, the aerodynamic forces change. The oscillations die out after around 2 seconds. Hence, no aeroelastic instabilities are encountered. It is expected that the lift and drag coefficient converge to the steady FSI values. This is the case for the lift coefficient. However, for the drag coefficient, the value converges to the value predicted without deformation. Due to the small difference, it is unclear whether this is physical or just explained by numerical inconsistencies such as different convergence levels between the simulations.

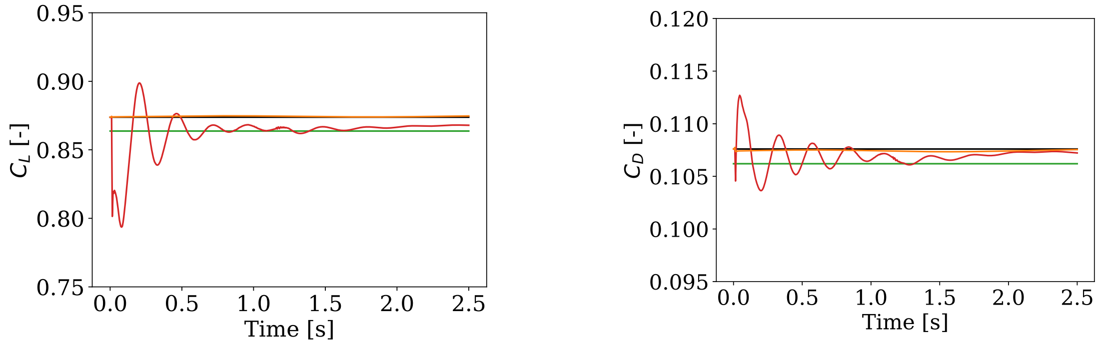

Figure 9: Lift and drag coefficient vs time. Black: steady CFD, green: steady FSI, red: unsteady FSI (two-way), orange: unsteady FSI (one-way).

A contour plot of the magnitude of deformation is given in Figure 10 for the steady FSI simulation. The deflection and twist deformation at the tip versus time is plotted in Figure 11 for the steady and unsteady FSI simulation. The unsteady FSI simulations (both two-way and one-way) converge to the steady FSI simulation after the oscillations die out. For the two-way simulation, the structural response is more damped due to the feedback of the aerodynamic loads to the structural deformation.

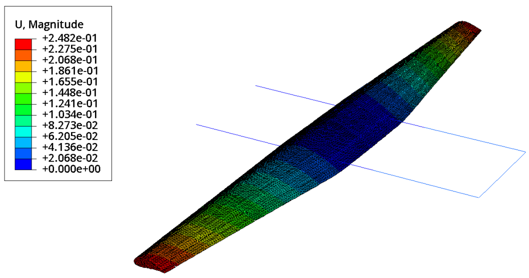

Figure 10: Magnitude of deformation in meter for the steady FSI simulation.

3.2 Steady crosswind flight condition

In this section, the results of the FSI simulations are presented for the crosswind flight condition. The simulations are initialized with an unsteady CFD simulation by simulating the aircraft motion before t=0 as indicated in Figure 12 (left). At t=0 the FSI simulation starts. On the right of Figure 12 the lift coefficient is plotted as a function of time. The results of the horizontal condition is plotted as well for comparison. The crosswind flight motion decreases the lift coefficient slightly. Besides, the results are similar to the horizontal case.
A contour plot of the magnitude of deformation is given in Figure 13 for the unsteady FSI simulation after the oscillations disappeared. The deflection and twist deformation at the tip versus time are plotted in Figure 14 for the steady and unsteady FSI simulation. The results are similar to the horizontal case. The main difference is the different deflection of the left and

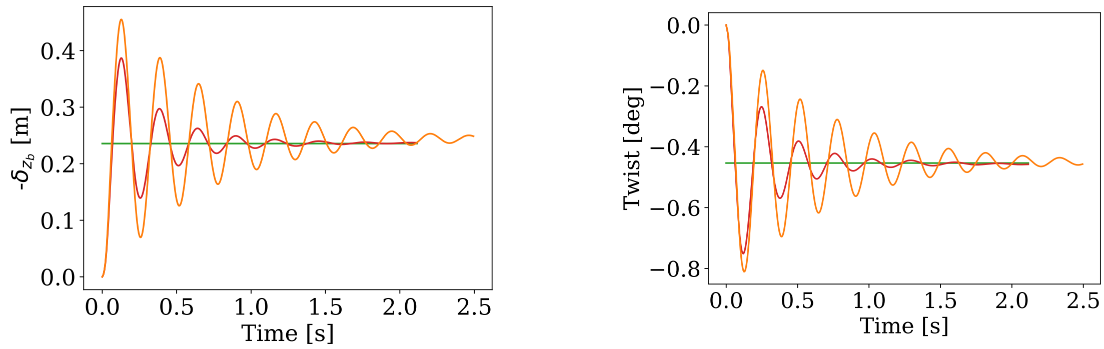

Figure 11: Deflection and twist deformation at tip vs. time. Green: steady FSI, red: unsteady FSI (two-way), orange: unsteady FSI (one-way).

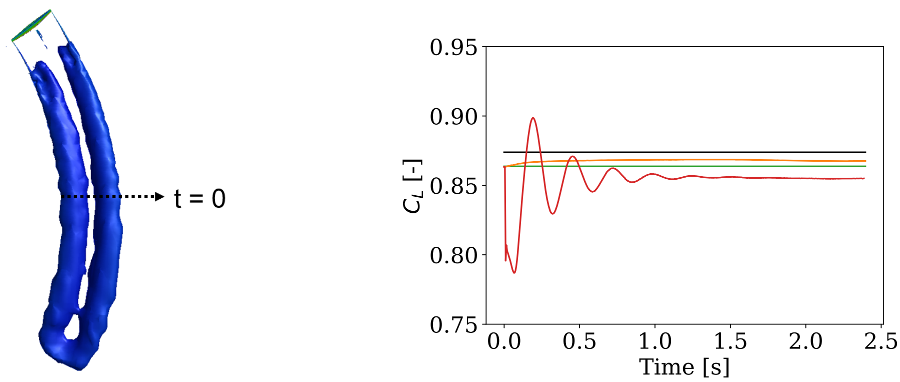

Figure 12: Visualization of wake and pressure contour (left). Lift coefficient vs time (right). Black: steady CFD (horizontal), green: steady FSI (horizontal), red: unsteady FSI (two-way), orange: unsteady FSI (one-way).

right wing. The right wing tip deforms more due to the higher experienced aerodynamic load. There is a difference of 12.6% in tip deflection between the left and right wing.

The unsteady FSI simulations in the crosswind flight conditions are performed using 39 cores for the aerodynamic model and 12 cores for the structural model on a 2x 20-core Intel Xeon Gold 6242R 3.1GHz system. The two-way and one-way approaches takes 75.0 and 74.8 hours respectively to complete a total simulation time of 2.5 seconds. Of this time 85% is used by the aerodynamic model, 10% by the structural model and 5% by the coupling procedure (both one-way and two-way).

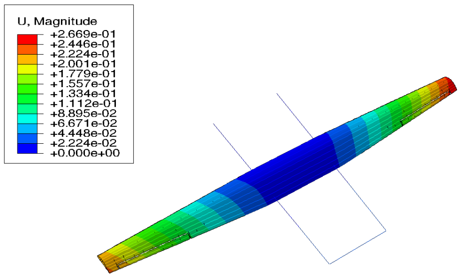

Figure 13: Magnitude of deformation for the unsteady FSI (two-way) simulation after oscillations disappeared.

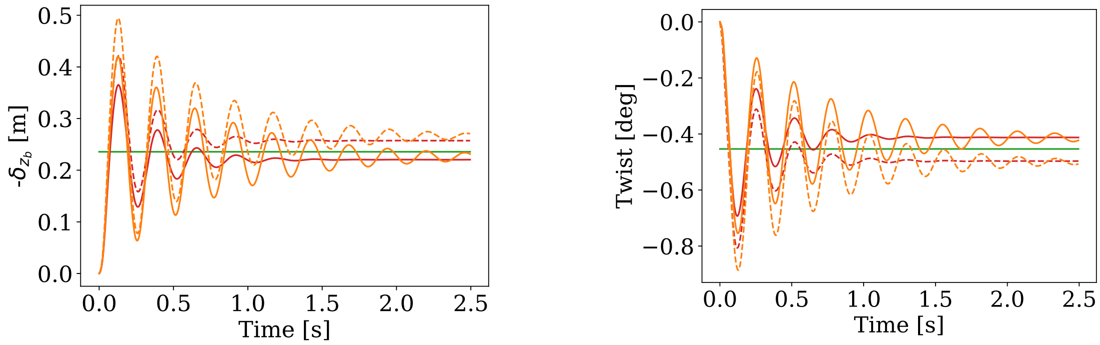

Figure 14: Deflection and twist deformation at tip vs. time. Green: steady FSI (horizontal), orange: unsteady FSI (one-way), red: unsteady FSI (two-way), solid line: left wing, dotted line: right wing.

4 CONCLUSIONS AND OUTLOOK

In this work a framework is presented that serves as a proof of concept to perform high fidelity simulations of airborne wind energy systems simulations. A technique has been developed to simulate the motion of an AWE aircraft and couple it with the structural model to perform high fidelity fluid-structure interaction simulations of an AWE system in crosswind flight. It has been found that the mesh deformation is sensitive to dynamic mesh parameters. On the other hand, the overset/Chimera technique has been proven to be a robust approach to simulate the motion of an AWE system in CFD simulations. This technique allows taking into account the large rigid body motion of the aircraft while maintaining a constant mesh quality. The first results revealed a reduction in lift coefficient of 1.4% due to a negative twist deflection of -0.45° for the multi-megawatt reference system flying at 80 m/s and 0° angle of attack. A difference in tip deflection between left and right of 12.6% is observed due to the circular motion. No aeroelastic instabilities have been encountered. The one-way FSI approach did not decrease the simulation time significantly compared to the two-way approach. Further refinements can be made by improving the overset connectivity and by including the rigid body motion in the structural model. Future work is directed toward coupling the FSI model with the body dynamics model presented in [7], in pursuit of physically feasible flight prediction and the accurate simulation of power production.

REFERENCES

[1] M. Diehl, Airborne wind energy: basic concepts and physical foundations, 2014.

[2] P. Echeverri, T. Fricke , G. Homsy and N. Tucker, The energy kite: selected results from the design, development and testing of Makani's airborne wind turbines, 2020.

[3] U. Fasel, D. Keidel, G. Molinari and P. Ermanni, Aeroservoelastic optimization of morphing airborne wind energy wings, *AIAA SciTech Forum*, San Diego, California, 2019.

[4] J. Wijnja, R. Schmehl, R. De Breuker, K. Jensen, D. Vander Lind, Aeroelastic analysis of a large airborne wind turbine, 2018.

[5] A. A. Candade, M. Ranneberg, R. Schmehl, Aero-structural design of composite wings for airborne wind energy applications, 2020.

[6] G. Santo, M. Peeters, W. Van Paepegem and J. Degroote , Dynamic load and stress analysis of a large horizontal axis wind turbine using full scale fluid-structure interaction simulation, *Renewable Energy*, 2019.

[7] K. Vimalakanthan, M. Caboni, J.G. Schepers, E. Pechenik, P. Williams, Aerodynamic analysis of Ampyx's airborne wind energy system, *Journal of Physics: Conference Series*, 1037 062008, 2018.

[8] M. Folkersma, R. Schmehl and A. Viré, Steady-state aeroelasticity of ram-air wing for airborne wind energy applications, 2020.

[9] T. Haas, J. De Schutter, M. Diehl, and J. Meyers, Large-eddy simulation of airborne wind energy farms, *Wind Energy Science*, 7, 1093–1135, https://doi.org/10.5194/wes-7-1093-2022, 2022.

[10] D. Eijkelhof, Design and optimization framework of a multi-MW airborne wind energy reference system (Master thesis), Delft University of Technology, Technical University of Denmark. 2019.

[11] J. Degroote, S. Annerel and J. Vierendeels, Stability analysis of Gauss-Seidel iterations in a partitioned simulation of fluid-structure interaction, *Computers & Structures*, vol. 88, no. 5–6, pp. 263–271, 2010.

[12] N. Pynaert, J. Wauters, G. Crevecoeur and J. Degroote, Unsteady aerodynamic simulations of a multi-megawatt airborne wind energy reference system using computational fluid dynamics, *Journal of Physics: Conference Series*, 2265 042060, 2022.

[13] J. Sorensen and W. Shen, Numerical modeling of wind turbine wakes, *Journal of Fluids Engineering* , 124, 393-399. http://dx.doi.org/10.1115/1.1471361, 2002.

[14] N. Delaissé, T. Demeester, D. Fauconnier and J. Degroote, Comparison of different quasi-Newton techniques for coupling of black box solvers, in ECCOMAS 2020, Proceedings, Paris, France, 2021.

[15] D. Eijkelhof, S. Rapp, U. Fasel, M. Gaunaa and R. Schmehl, Reference design and simulation framework of a multi-megawatt airborne wind energy system, *Journal of Physics Conference Series*, 2020.